Chain and Large-Ring Polymeric Transition Metal and Lanthanide Complexes Formed by *N,N'*-Ethylenebis(pyrrolidin-2-one)

Garry A. Doyle, David M. L. Goodgame,* Stuart P. W. Hill, Stephan Menzer, Alistair Sinden, and David J. Williams

Chemistry Department, Imperial College of Science, Technology and Medicine,
London SW7 2AY, U.K.

Received December 7, 1994®

With the aim of exploring the types of polymeric structures generated by the "extended reach" ligand *N,N'*-ethylenebis(pyrrolidin-2-one) (ebpyrr), a range of complexes with $\mathrm{Mn^{II}}$, $\mathrm{Fe^{III}}$, $\mathrm{Co^{II}}$, $\mathrm{Ni^{II}}$, $\mathrm{Cu^{II}}$, $\mathrm{Zn^{II}}$, lanthanide ions, and $\mathrm{Th^{IV}}$ have been isolated, and five representative members have been structurally characterized by X-ray crystallography. $[\mathrm{Co(ebpyrr)Cl_2}]_n$ crystallizes in the monoclinic space group $P2_1/n$, with $a = 9.827(4)$ Å, $b = 9.369(3)$ Å, $c = 14.747(7)$ Å, $\beta = 94.13(2)°$, and $V = 1354.2(9)$ Å^3 for $Z = 4$. $[\mathrm{Zn(ebpyrr)I_2}]_n$ crystallizes in the monoclinic space group Cc, with $a = 9.013(4)$ Å, $b = 15.967(6)$ Å, $c = 11.002(4)$ Å, $\beta = 103.76(2)°$, and $V = 1537.9(11)$ Å^3 for $Z = 4$. Both these complexes contain tetrahedrally coordinated metal ions linked by ebpyrr bridges to form chains. $[\mathrm{Co(ebpyrr)(NO_3)_2(MeCN)}]_n$ crystallizes in the monoclinic space group $C2/c$, with $a = 31.53(6)$ Å, $b = 8.242(8)$ Å, $c = 14.99(2)$ Å, $\beta = 115.3(1)°$, and $V = 3522(9)$ Å^3 for $Z = 8$. Chains are also formed by this complex, but in this case the metal ion is octahedrally coordinated. $\mathrm{Cd(ebpyrr)_2(NO_3)_2{\cdot}H_2O}$ crystallizes in the monoclinic space group $C2/c$, with $a = 13.907(6)$ Å, $b = 11.927(5)$ Å, $c = 17.076(8)$ Å, $\beta = 109.71(2)°$, and $V = 2666(2)$ Å^3 for $Z = 4$. The cadmium atom in this mononuclear complex adopts an essentially pentagonal bipyramidal coordination geometry with two oxygen atoms, one from each of the two ebpyrr molecules, occupying the axial positions and two chelating nitrate groups and the aqua ligand forming the equatorial plane. The monomers are linked via hydrogen bonds to form sheets. $[\mathrm{Zn(ebpyrr)_3](ClO_4)_2{\cdot}2MeCN}$ crystallizes in the triclinic space group $P\bar{1}$, with $a = 7.533(2)$ Å, $b = 10.788(4)$ Å, $c = 13.014(4)$ Å, $\alpha = 98.79(2)°$, $b = 92.32(2)°$, $\gamma = 98.77(2)°$, and $V = 1030.7(6)$ Å^3 for $Z = 1$. This compound also forms sheets but here the linkages are covalent, via ebpyrr bridges, and the structure contains both 18- and 36-membered rings.

Introduction

We are currently studying the use of bis(pyridones) **I**, bis(lactams) **II**, and related ligands to produce complexes with unusual polymeric structures, and we have described some examples of the various types of compounds that can be obtained.[1-7,8a] In the specific case of the ethylene-bridged bis(lactam) ligand *N,N'*-ethylenebis(pyrrolidin-2-one) (**III**, ebpyrr), sheets of contiguous 54-membered metallomacrocyclic rings were found in the erbium(III) nitrate complex $[\mathrm{Er_2(ebpyrr)_3(NO_3)_6}]_n$,[1] whereas uranyl nitrate gave a helical-chain polymer $[\mathrm{UO_2(ebpyrr)(NO_3)_2}]_n$ and also a dinuclear μ-η^2,η^2-peroxo-bridged complex $\{[\mathrm{UO_2(ebpyrr)(NO_3)}]_2(\mu\text{-}\mathrm{O_2})\}$.[3] To explore yet further the structural diversity available with ligands of this type, we have investigated the complexes formed by **III** with a wide range of metal ions. We report here the types of complex that we have obtained and give the results of full X-ray characterization of five of them, namely the complexes $\mathrm{CoCl_2(ebpyrr)}$ (**1**), $\mathrm{ZnI_2(ebpyrr)}$ (**2**), $\mathrm{Co(ebpyrr)(NO_3)_2(MeCN)}$ (**3**), $[\mathrm{Zn(ebpyrr)_3](ClO_4)_2{\cdot}2MeCN}$ (**4**), and $\mathrm{Cd(ebpyrr)_2(NO_3)_2{\cdot}H_2O}$ (**5**).

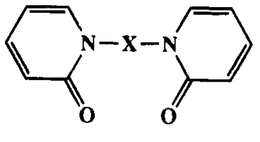

I

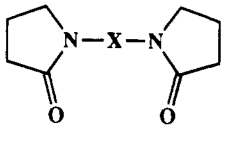

II

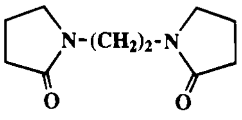

III

Experimental Section

Preparation of Compounds. ***N,N'*-Ethylenebis(pyrrolidin-2-one) (ebpyrr).** This was prepared by a literature method[8b] but extracted from the crude product with isooctane.

Metal Complexes of epbyrr. The metal complexes were obtained by reacting ebpyrr and the appropriate metal salt (AR or reagent grade) in 2:1 mole ratio in an organic solvent (acetonitrile, 2,2-dimethoxypropane, ethanol, or methanol) or a mixture of solvents. The compounds either precipitated immediately or crystallized on slow concentration of the

---

® Abstract published in *Advance ACS Abstracts,* May 1, 1995.

(1) Doyle, G. A.; Goodgame, D. M. L.; Hill, S. P. W.; Williams, D. J. *J. Chem. Soc., Chem. Commun.* **1993**, 207.
(2) Goodgame, D. M. L.; Hill, S. P. W.; Williams, D. J. *J. Chem. Soc., Chem. Commun.* **1993**, 1019.
(3) Doyle, G. A.; Goodgame, D. M. L.; Sinden, A.; Williams, D. J. *J. Chem. Soc., Chem. Commun.* **1993**, 1170.
(4) Goodgame, D. M. L.; Hill, S. P. W.; Williams, D. J. *Polyhedron* **1993**, *12*, 2933.
(5) Goodgame, D. M. L.; Hill, S. P. W.; Smith, A. M.; Williams, D. J. *J. Chem. Soc., Dalton Trans.* **1994**, 859.
(6) Goodgame, D. M. L.; Menzer, S.; Smith, A. M.; Williams, D. J. *J. Chem. Soc., Chem. Commun.* **1994**, 1825.
(7) Goodgame, D. M. L.; Menzer, S.; Ross, A. T.; Williams, D. J. *J. Chem. Soc., Chem. Commun.* **1994**, 2605.
(8) (a) Goodgame, D. M. L.; Menzer, S.; Smith, A. M.; Williams, D. J. *Inorg. Chem.* **1994**, *33*, 6409. (b) Reppe, W. *Liebigs Ann. Chem.* **1955**, *596*, 1. (c) Carrad, L. H.; Goodgame, D. M. L.; Hill, S. P. W.; Williams, D. J. *J. Chem. Soc., Dalton Trans.* **1993**, 1003.

0020-1669/95/1334-2850$09.00/0

Table 1. Crystallographic Data for $CoCl_2$(ebpyrr) (**1**), ZnI_2(ebpyrr) (**2**), Co(ebpyrr)$(NO_3)_2$(MeCN) (**3**), [Zn(ebpyrr)$_3$]$(ClO_4)_2{\cdot}$2MeCN (**4**), and Cd(ebpyrr)$_2(NO_3)_2{\cdot}H_2O$ (**5**)

	1	2	3	4	5
formula	$C_{10}H_{16}Cl_2CoN_2O_2$	$C_{10}H_{16}I_2N_2O_2Zn$	$C_{12}H_{19}CoN_5O_8$	$C_{34}H_{54}Cl_2N_8O_{14}Zn$	$C_{20}H_{34}CdN_6O_{11}$
fw	326.1	515.4	420.3	935.1	646.9
space group	$P2_1/n$	Cc	$C2/c$	$P\bar{1}$	$C2/c$
a, Å	9.827(4)	9.013(4)	31.53(6)	7.533(2)	13.907(6)
b, Å	9.369(3)	15.967(6)	8.242(8)	10.788(4)	11.927(5)
c, Å	14.747(7)	11.002(4)	14.99(2)	13.014(4)	17.076(8)
α, deg				98.79(2)	
β, deg	94.13(2)	103.76(2)	115.3(1)	92.32(2)	109.71(2)
γ, deg				98.77(2)	
V, Å^3	1354.2(9)	1537.9(11)	3522(9)	1030.7(6)	2666(2)
Z	4	4	8	1	4
ϱ_{calcd}, g cm^{-3}	1.599	2.226	1.585	1.506	1.611
λ, Å	1.541 78	0.710 73	0.710 73	1.541 78	0.710 73
μ, cm^{-1}	135.1	56.1	10.3	26.7	8.9
T, °C	24	24	24	24	24
R^a	0.0518	0.0261	0.0654	0.0489	0.0379
R$_w{}^b$	0.0474	0.0314	0.1540^c	0.1308^c	0.0386

^{a} $R = \Sigma|F_o - F_c|/\Sigma|F_o|$. ^{b} $R_w = \Sigma[|F_o - F_c|w^{1/2}]/\Sigma[|F_o|w^{1/2}]$; $w^{-1} = [\sigma^2(F_o) + g(F_o{}^2)]$. ^{c} w$R_2$ (SHELXL-93).

solutions at room temperature. The solid products were collected, washed with a small amount of the solvent used for the reaction, and either air-dried or dried *in vacuo* over silica gel or P_2O_5. Relevant specific details and analytical data (Microanalytical Laboratory, Imperial College) are summarized below.

$Mn(NO_3)_2(ebpyrr)_2{\cdot}H_2O$: White, fibrous, hygroscopic solid from acetonitrile (38% yield). Anal. Calc for $C_{20}H_{34}MnN_6O_{11}$: C, 40.8; H, 5.8; N, 14.3. Found: C, 40.8; H, 5.6; N, 13.8.

$Mn(ClO_4)_2(ebpyrr)_3$: *Caution! Metal perchlorates are potentially explosive* (see, for example: *J. Chem. Educ.* **1973**, *50*, A335). A white powder was obtained from acetonitrile (62% yield). Anal. Calc for $C_{30}H_{48}Cl_2MnN_6O_{14}$: C, 42.8; H, 5.7; N, 10.0. Found: C, 42.3; H, 5.7; N, 10.3.

$FeCl_3(ebpyrr)$: Orange powder from methanol; ν(Fe$-$Cl) 379 cm^{-1}. Anal. Calc for $C_{10}H_{16}Cl_3FeN_2O_2$: C, 33.5; H, 4.5; N, 7.8. Found: C, 33.5; H, 4.7; N, 7.6.

$Co(NO_3)_2(ebpyrr){\cdot}CH_3CN$: Magenta, hygroscopic needles from acetonitrile/2,2-dimethoxypropane (80% yield as microcrystalline powder; yield of crystals grown for X-ray study not measured). Anal. Calc for $C_{12}H_{19}CoN_5O_8$: C, 34.3; H, 4.6; N, 16.7. Found: C, 33.4; H, 4.4; N, 16.1.

$CoCl_2(ebpyrr){\cdot}H_2O$: Dark blue platelike crystals from methanol/2,2-dimethoxypropane (86% yield); ν(Co$-$Cl) 343, 304 cm^{-1}. Anal. Calc for $C_{10}H_{18}Cl_2CoN_2O_3$: C, 34.9; H, 5.3; N, 8.1. Found: C, 34.8; H, 4.6; N, 8.1.

$CoBr_2(ebpyrr)$: Dark blue powder from methanol/2,2-dimethoxypropane (80% yield). Anal. Calc for $C_{10}H_{16}Br_2CoN_2O_2$: C, 28.9; H, 3.9; N, 6.75. Found: C, 29.0; H, 3.7; N, 6.7.

$CoI_2(ebpyrr)$: Dark blue powder from ethanol/2,2-dimethoxypropane (78% yield). Anal. Calc for $C_{10}H_{16}CoI_2N_2O_2$: C, 23.6; H, 3.2; N, 5.5. Found: C, 23.5; H, 3.0; N, 5.7.

$Ni(NO_3)_2(ebpyrr){\cdot}H_2O$: Apple-green, hygroscopic powder from 2,2-dimethoxypropane (81% yield). Anal. Calc for $C_{10}H_{18}NiN_4O_9$: C, 30.25; H, 4.6; N, 14.1. Found: C, 30.5; H, 4.6; N, 13.9.

$Cu(NO_3)_2(ebpyrr)$: Sky blue, hygroscopic powder from 2,2-dimethoxypropane (65% yield). Anal. Calc for $C_{10}H_{16}CuN_4O_8$: C, 31.3; H, 4.6; N, 14.6. Found: C, 31.4; H, 4.6; N, 14.5.

$Zn(NO_3)_2(ebpyrr)$: White, hygroscopic powder from 2,2-dimethoxypropane (58% yield). Anal. Calc for $C_{10}H_{16}N_4O_8Zn$: C, 31.1; H, 4.2; N, 14.5. Found: C, 30.8; H, 4.1; N, 14.4.

$ZnCl_2(ebpyrr){\cdot}0.5H_2O$: White microcrystalline clusters from methanol/2,2-dimethoxypropane (79% yield); ν(Zn$-$Cl) 338, 302 cm^{-1}. Anal. Calc for $C_{10}H_{17}Cl_2N_2O_{2.5}Zn$: C, 35.3; H, 5.0; N, 8.2. Found: C, 35.2; H, 4.7; N, 8.0.

$ZnBr_2(ebpyrr)$: White microcrystalline clusters from methanol/2,2-dimethoxypropane (83% yield). Anal. Calc for $C_{10}H_{16}Br_2N_2O_2Zn$: C, 28.5; H, 3.8; N, 6.65. Found: C, 28.3; H, 3.7; N, 6.4.

$ZnI_2(ebpyrr)$: Colorless prisms from ethanol/2,2-dimethoxypropane (67% yield). Anal. Calc for $C_{10}H_{16}I_2N_2O_2Zn$: C, 23.3; H, 3.1; N, 5.7. Found: C, 23.7; H, 2.9; N, 5.7.

$Zn(ClO_4)_2(ebpyrr)_3$: *Caution! Metal perchlorates are potentially explosive* (see, for example: *J. Chem. Educ.* **1973**, *50*, A335). Colorless blocklike crystals were obtained from acetonitrile (47% yield). Anal. Calc for $C_{30}H_{48}Cl_2N_6O_{14}Zn$: C, 42.2; H, 5.7; N, 9.85. Found: C, 41.8; H, 5.7; N, 10.15.

$Zn(BF_4)_2(ebpyrr)_3{\cdot}CH_3CN$: Colorless crystals from acetonitrile (35% yield). Anal. Calc for $C_{32}H_{51}B_2F_8N_7O_6Zn$: C, 44.2; H, 5.9; N, 11.3. Found: C, 43.9; H, 5.95; N, 11.8.

$Cd_2(NO_3)_4(ebpyrr)_3$: White needles from 2,2-dimethoxypropane (35% yield). Anal. Calc for $C_{30}H_{48}Cd_2N_{10}O_{18}$: C, 33.9; H, 4.6; N, 13.2. Found: C, 33.9; H, 4.7; N, 12.8.

$Cd(NO_3)_2(ebpyrr)_2{\cdot}H_2O$: Colorless crystals of this complex were obtained from attempts to grow X-ray quality crystals of the previous compound using the following method. The organic ligand (78 mg) was dissolved in 5 mL of acetonitrile containing 2 drops of water, followed by addition of $Cd(NO_3)_2{\cdot}4H_2O$ (62 mg). The resulting solution was transferred to a Young's tube which was then sealed. The colorless crystals which formed overnight were characterized by X-ray diffraction.

$M_2(NO_3)_6(ebpyrr)_3$ Where M = Y or a Lanthanide Ion Pr$-$Yb. As outlined in the Discussion, a range of solvents can be used to prepare these complexes. The following details are for samples crystallized from acetonitrile followed by desolvation *in vacuo*.

M = Y: Colorless (76% yield). Anal. Calc for $C_{30}H_{48}N_{12}O_{24}Y_2$: C, 31.6; H, 4.2; N, 14.8. Found: C, 31.5; H, 4.1; N, 14.5.

M = Pr: Green (52% yield). Anal. Calc for $C_{30}H_{48}N_{12}O_{24}Pr_2$: C, 29.0; H, 3.9; N, 13.5. Found: C, 28.5; H, 3.8; N, 13.3.

M = Nd: Lilac (52% yield). Anal. Calc for $C_{30}H_{48}N_{12}Nd_2O_{24}$: C, 28.8; H, 3.9; N, 13.5. Found: C, 29.3; H, 3.9; N, 13.7.

M = Sm: Colorless (56% yield). Anal. Calc for

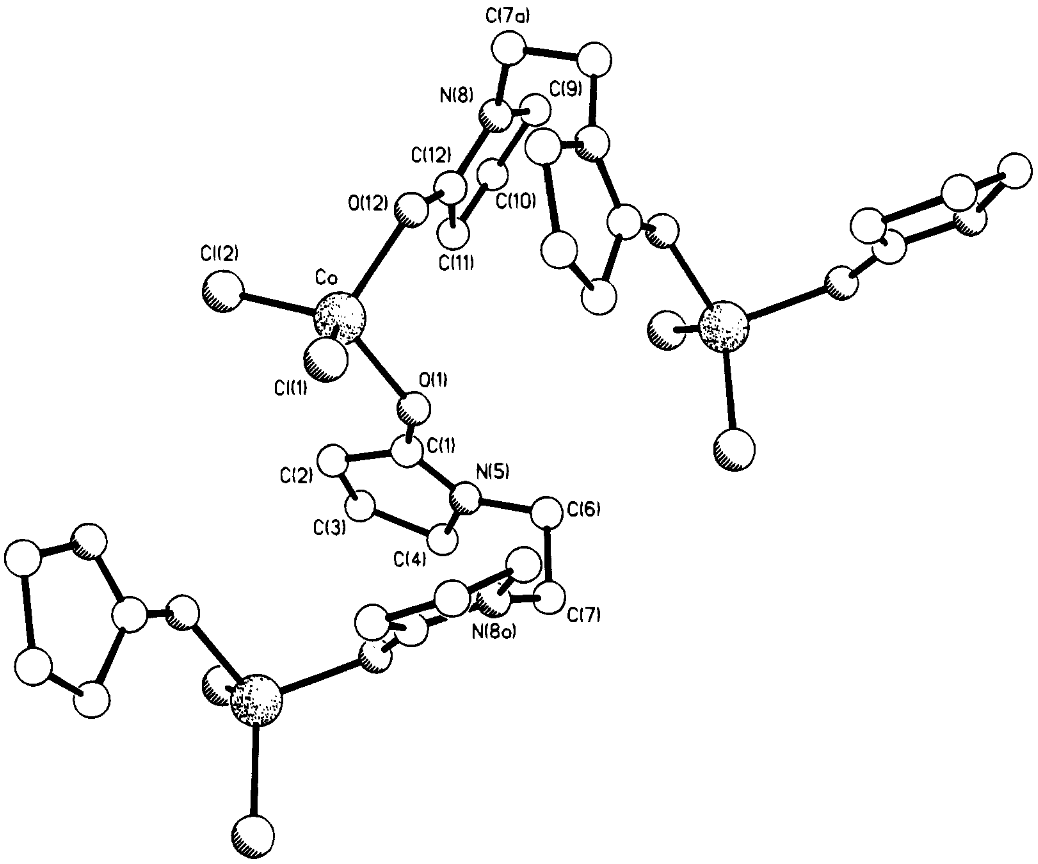

Figure 1. Part of the helical chain structure formed by **1**, showing the crystallographic numbering scheme.

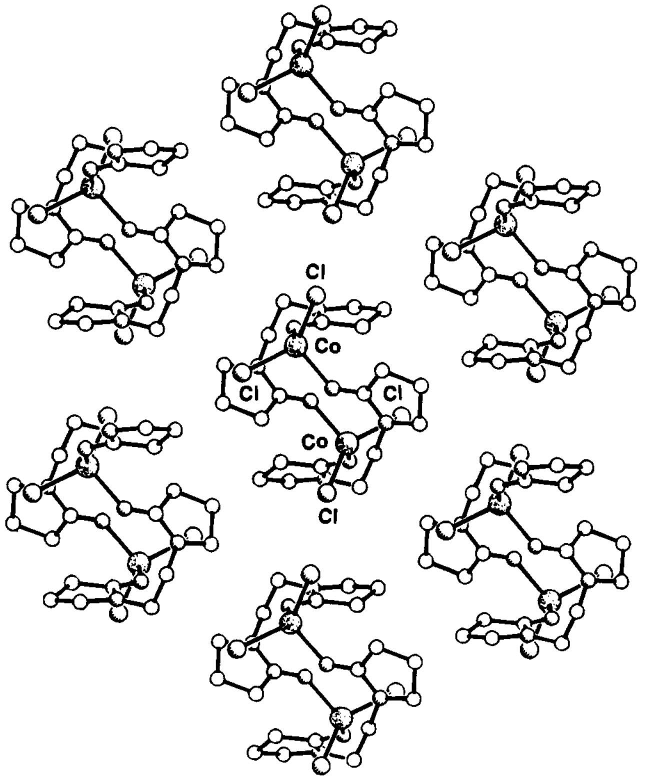

Figure 2. Hexagonal close-packing of the helical chains in the crystal structure of **1**.

$C_{30}H_{48}N_{12}O_{24}Sm_2$: C, 28.6; H, 3.8; N, 13.3. Found: C, 28.7; H, 3.75; N, 13.3.

M = Eu: Colorless (55% yield). Anal. Calc for $C_{30}H_{48}Eu_2N_{12}O_{24}$: C, 28.5; H, 3.8; N, 13.3. Found: C, 29.0; H, 3.8; N, 13.5.

M = Gd: Colorless (78% yield). Anal. Calc for $C_{30}H_{48}Gd_2N_{12}O_{24}$: C, 28.25; H, 3.8; N, 13.2. Found: C, 28.6; H, 3.7; N, 13.1.

M = Tb: Colorless (90% yield). Anal. Calc for $C_{30}H_{48}N_{12}O_{24}Tb_2$: C, 28.2; H, 3.8; N, 13.15. Found: C, 28.2; H, 3.6; N, 13.2.

M = Dy: Colorless (60% yield). Anal. Calc for $C_{30}H_{48}Dy_2N_{12}O_{24}$: C, 28.0; H, 3.8; N, 13.1. Found: C, 27.7; H, 3.6; N, 12.8.

M = Ho: Pink (58% yield). Anal. Calc for $C_{30}H_{48}Ho_2N_{12}O_{24}$: C, 27.9; H, 3.75; N, 13.0. Found: C, 27.9; H, 3.6; N, 12.9.

M = Er: Pink (60% yield). Anal. Calc for $C_{30}H_{48}Er_2N_{12}O_{24}$: C, 27.8; H, 3.7; N, 13.0. Found: C, 28.1; H, 3.6; N, 13.05.

M = Tm: White (58% yield). Anal. Calc for $C_{30}H_{48}N_{12}O_{24}Tm_2$: C, 27.7; H, 3.7; N, 12.95. Found: C, 27.7; H, 3.6; N, 13.0.

M = Yb: White (63% yield). Anal. Calc for $C_{30}H_{48}N_{12}O_{24}Yb_2$: C, 27.6; H, 3.7; N, 12.9. Found: C, 27.9; H, 3.6; N, 13.0.

$Th_2(NO_3)_8(ebpyrr)_3$: Fine white powder from ethanol (71% yield). Anal. Calc for $C_{30}H_{48}N_{14}O_{30}Th_2$: C, 23.3; H, 3.1; N, 12.7. Found: C, 23.3; H, 2.8; N, 12.3.

Spectroscopy: Spectroscopic measurements were made as described previously.[8c]

Crystallographic Analysis. Crystal data for $CoCl_2(ebpyrr)$ (**1**), $ZnI_2(ebpyrr)$ (**2**), $Co(ebpyrr)(NO_3)_2(MeCN)$ (**3**), $[Zn(ebpyrr)_3](ClO_4)_2\cdot 2MeCN$ (**4**), and $Cd(ebpyrr)_2(NO_3)_2\cdot H_2O$ (**5**) and a summary of the crystallographic analysis are given in Table 1. The data were collected on a Siemens P4 diffractometer using ω-scans and graphite-monochromated Cu Kα radiation for **1** and **4** and Mo Kα radiation for **2**, **3**, and **5**. The data were corrected for Lorentz and polarization factors and for absorption.

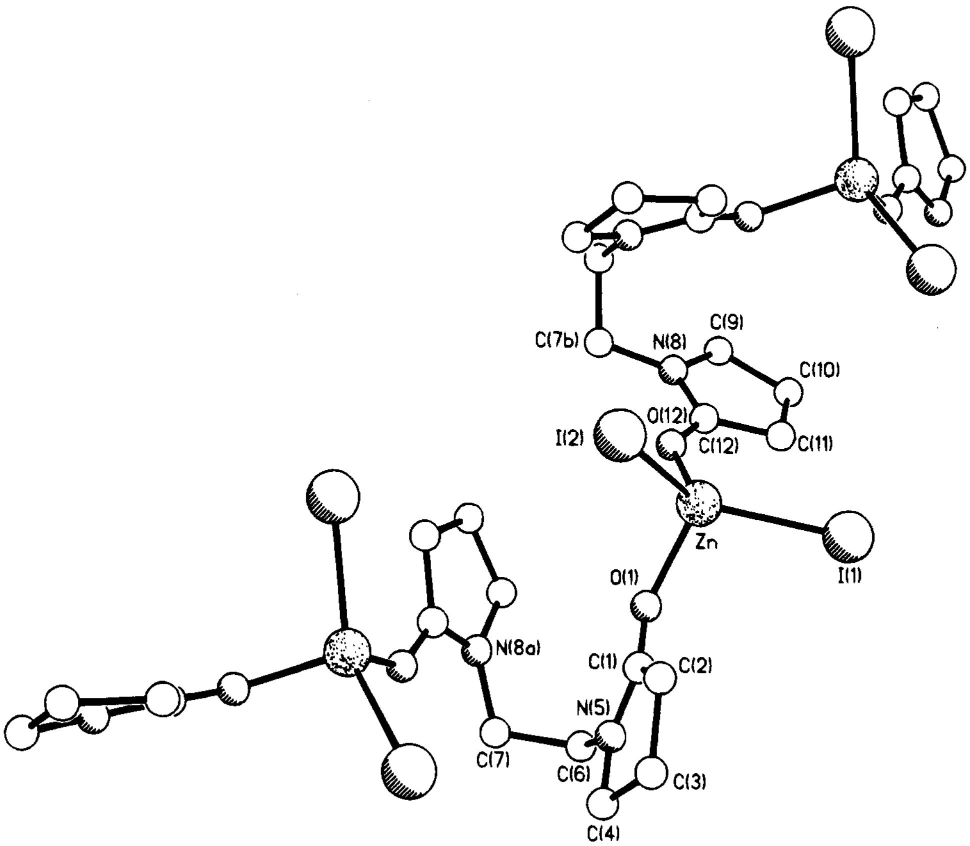

Figure 3. Part of the chain structure formed by **2**, showing the crystallographic numbering scheme.

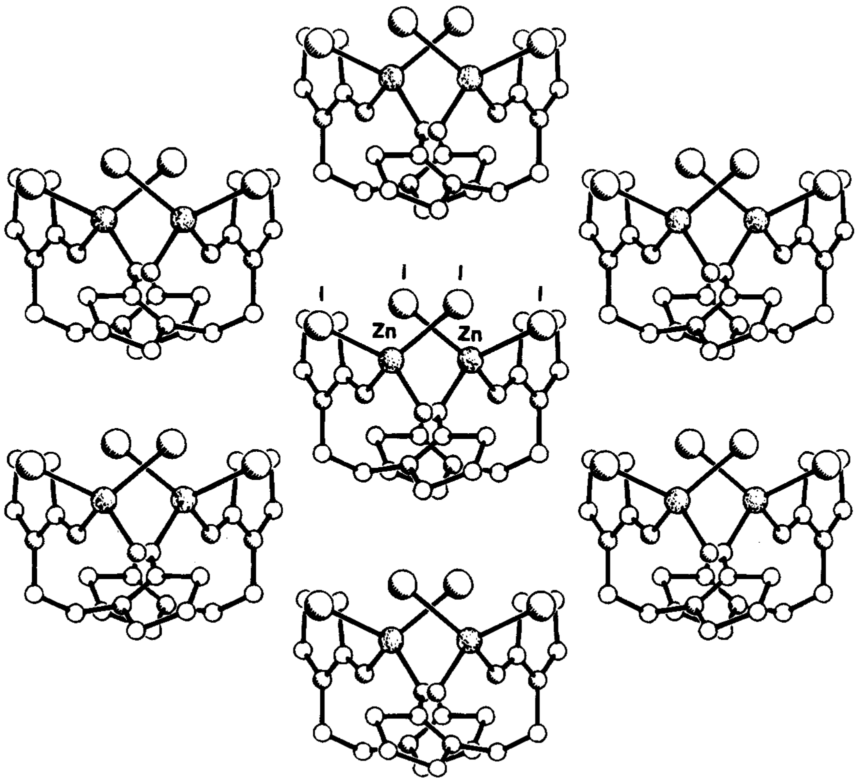

Figure 4. Flattened hexagonal close-packing of the helical chains in the crystal structure of compound **2**, illustrating the polar nature of the structure.

All the structures were solved by direct methods and their non-hydrogen atoms refined anisotropically with the exception of the structure of **3**. In the case of **3**, after three attempts a partial data set was obtained before the crystal decomposed. Consequently, because of the severely limited number of observed data, only the cobalt atom was allowed to refine anisotropically, the remaining non-hydrogen atoms being refined isotropically. For all the structures the hydrogen atoms were placed in calculated positions, assigned isotropic thermal parameters $U(\mathrm{H}) = 1.2U_{\mathrm{eq}}(\mathrm{C})$, and allowed to ride on their parent carbon atoms. In **5** the hydrogen atoms of the aqua ligand were located from a ΔF map and refined isotropically subject to an O$-$H distance

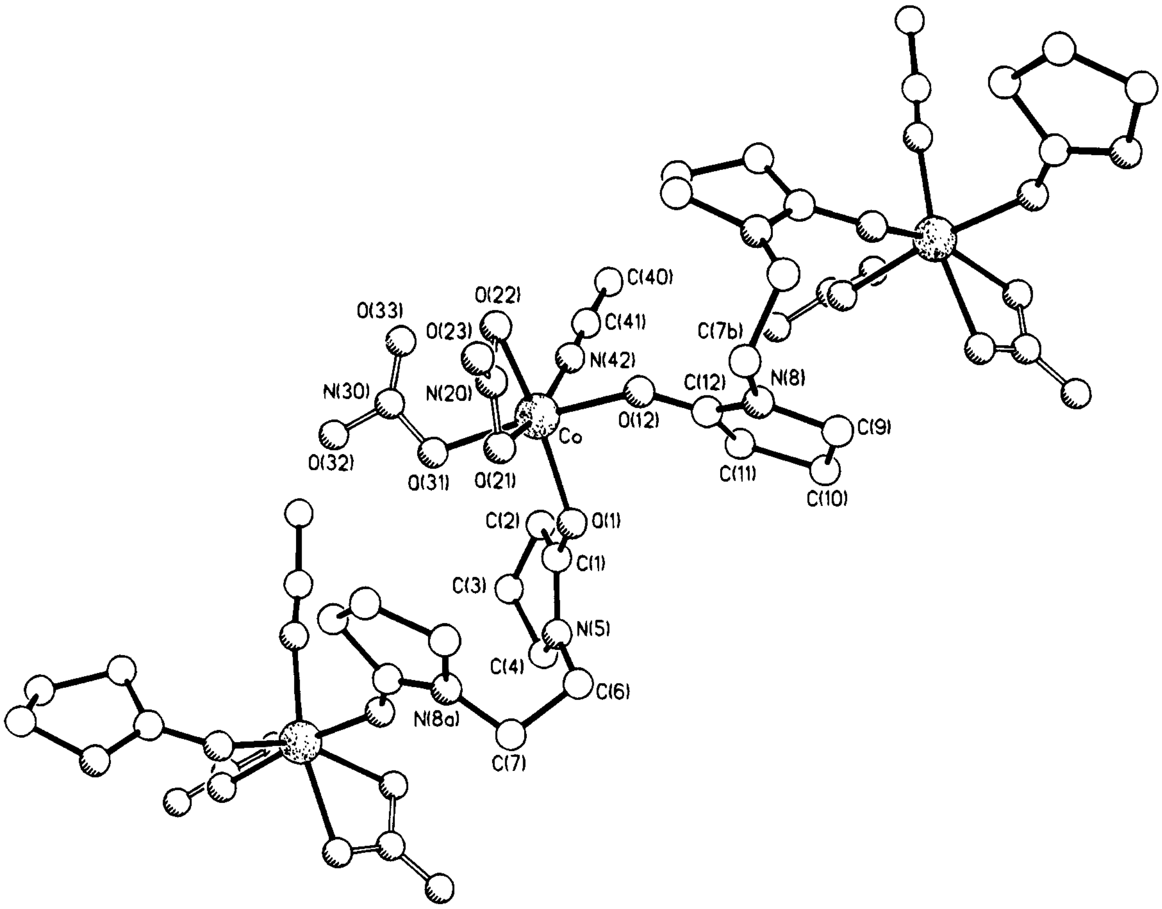

Figure 5. Part of the chain structure formed by **3**, showing the crystallographic numbering scheme.

constraint. Refinements were by full-matrix least squares; those for **3** and **4** were based on F^2 and those for the remainder on F. The polarity of **2** was determined by an η refinement. This parameter refined to a value of 1.16(11), providing a definitive assignment for the crystal selected.

Computations were carried out on 486 PCs using the SHELXTL PC system[9a] or the SHELXL-93 program.[9b] Fractional atomic coordinates and equivalent isotropic displacement coefficients for structures **1**–**5** are given in Tables 2–6 and selected bond lengths and angles in Tables 7–11.

Results and Discussion

As our main aim in this work was to investigate the ability of **III** to generate polymeric compounds, we have concentrated on attempting to isolate solid materials suitable for full characterization by single-crystal X-ray diffraction studies. Where this could not be achieved, some limited information about the immediate coordination environment of the metal ions was obtained by spectroscopic methods.

Although **III** gave a wide range of solid complexes, as summarized in the Experimental Section, the formation of crystals of appropriate quality was found to be critically dependent on the solvent employed. This may be exemplified for the complex $[Er_2(ebpyrr)_3(NO_3)_6]_n$ (**6**), the structure of which has been described in a preliminary communication.[1] This complex may be obtained in virtually quantitative yield from nitromethane (in good crystalline form) or from 2,2-dimethoxypropane (but only as a finely divided powder). Good crystals were also obtained from acetonitrile or butan-1-ol, but the yields were lower (ca. 60%).

Table 2. Atomic Coordinates ($\times 10^4$) and Equivalent Isotropic Displacement Coefficients (Å^2 × 10^3) for **1**

	x	y	z	U(eq)[a]
Co	4171(1)	2276(1)	1859(1)	39(1)
Cl(1)	3020(2)	1692(3)	560(1)	61(1)
Cl(2)	6017(2)	1021(2)	2317(2)	64(1)
O(1)	2757(4)	2340(5)	2749(3)	43(2)
C(1)	2665(7)	1767(8)	3525(5)	35(3)
C(2)	3568(7)	635(9)	3946(6)	60(4)
C(3)	3124(8)	495(9)	4900(5)	55(3)
C(4)	1773(8)	1255(10)	4885(5)	58(4)
N(5)	1697(6)	2086(6)	4066(4)	34(2)
C(6)	548(7)	3004(8)	3812(5)	40(3)
C(7)	−694(7)	2148(8)	3471(5)	37(3)
N(8)	5513(6)	6432(6)	2378(4)	33(2)
C(9)	5734(8)	7166(8)	3257(5)	47(3)
C(10)	5750(9)	5979(9)	3950(5)	55(3)
C(11)	5061(8)	4744(9)	3458(5)	48(3)
C(12)	5100(8)	5096(9)	2461(5)	41(3)
O(12)	4793(5)	4285(5)	1801(3)	43(2)

[a] Equivalent isotropic U defined as one-third of the trace of the orthogonalized U_{ij} tensor.

Another characteristic property of many of these compounds is their tendency to take up solvent molecules, but these are frequently rapidly lost on removal of the crystals from their mother liquor, generally resulting in loss of crystallinity. Thus compound **6** forms solvates with acetonitrile, butan-1-ol, or nitromethane, but with acetonitrile the solvent molecules are quite readily lost after crystal isolation, and we observed no solvation with 2,2-dimethoxypropane. Solvent inclusion and its subsequent loss after crystal isolation therefore strongly

---

(9) (a) Sheldrick, G. M. *SHELXTL PC*, Version 4.2; Siemens Analytical Instruments Inc.: Madison, WI, 1990. (b) Sheldrick, G. M. *SHELXL-93*; University of Göttingen: Göttingen, Germany, 1993.

Table 3. Atomic Coordinates ($\times 10^4$) and Equivalent Isotropic Displacement Coefficients (Å^2 $\times$ 10^3) for **2**

	x	*y*	*z*	*U*(eq)^a
Zn	4120(1)	8191(1)	9546(1)	35(1)
I(1)	2344	9450(1)	8992	48(1)
I(2)	3555(1)	7018(1)	10970(1)	59(1)
O(1)	6180(5)	8662(3)	10339(4)	40(1)
C(1)	6546(6)	9025(3)	11366(4)	34(1)
C(2)	5607(8)	9109(5)	12324(6)	54(2)
C(3)	6491(9)	9713(5)	13290(6)	57(2)
C(4)	8084(9)	9749(4)	13067(5)	49(2)
N(5)	7872(6)	9394(3)	11802(4)	34(1)
C(6)	9129(6)	9392(3)	11184(5)	34(1)
C(7)	10248(5)	8678(3)	11607(5)	34(1)
N(8)	4546(5)	7117(3)	6183(4)	33(1)
C(9)	4131(7)	7346(4)	4860(4)	43(2)
C(10)	3481(15)	8221(5)	4863(7)	73(3)
C(11)	3589(13)	8444(4)	6194(6)	60(3)
C(12)	4301(7)	7713(3)	6930(5)	38(1)
O(12)	4630(7)	7631(3)	8096(4)	54(1)

^{a} Equivalent isotropic *U* defined as one−third of the trace of the orthogonalized $\mathbf{U}_{ij}$ tensor.

Table 4. Atomic Coordinates ($\times 10^4$) and Equivalent Isotropic Displacement Coefficients (Å^2 $\times$ 10^3) for **3**

	x	*y*	*z*	*U*(eq)^a
Co	−1324(1)	−1507(2)	−193(1)	79(2)
O(1)	−1049(5)	616(11)	−453(6)	75(3)
C(1)	−1250(8)	1678(16)	−1100(9)	63(4)
C(2)	−1743(9)	2069(19)	−1636(11)	91(5)
C(3)	−1776(8)	3061(19)	−2516(10)	88(5)
C(4)	−1300(7)	3779(18)	−2185(10)	81(5)
N(5)	−990(8)	2609(14)	−1439(8)	75(4)
C(6)	−497(8)	2630(19)	−1041(11)	81(5)
C(7)	−303(8)	2035(17)	−1782(10)	83(5)
N(8)	−469(6)	−418(13)	2830(7)	72(3)
C(9)	−331(7)	1029(17)	3442(11)	90(5)
C(10)	−584(8)	2363(20)	2757(11)	101(6)
C(11)	−933(7)	1612(16)	1815(10)	83(5)
C(12)	−801(7)	−148(16)	1945(9)	70(4)
O(12)	−974(5)	−1223(11)	1315(6)	77(3)
N(20)	−865(9)	−4196(17)	309(9)	82(5)
O(21)	−718(5)	−3001(12)	−45(6)	78(3)
O(22)	−1276(7)	−4069(12)	230(7)	84(4)
O(23)	−615(6)	−5391(15)	660(8)	114(4)
N(30)	−1954(8)	−2592(18)	−2199(11)	99(5)
O(31)	−1571(6)	−1818(14)	−1710(8)	106(4)
O(32)	−2072(6)	−2704(13)	−3090(8)	102(4)
O(33)	−2137(7)	−3317(17)	−1773(10)	134(5)
N(42)	−1942(9)	−637(20)	−135(10)	94(6)
C(41)	−2248(9)	−338(23)	−45(11)	78(6)
C(40)	−2669(8)	196(20)	49(10)	90(6)

^{a} Equivalent isotropic *U* defined as one-third of the trace of the orthogonalized $\mathbf{U}_{ij}$ tensor.

Table 5. Atomic Coordinates ($\times 10^4$) and Equivalent Isotropic Displacement Coefficients (Å^2 $\times$ 10^3) for **4**

	x	*y*	*z*	*U*(eq)^a
Zn	0	0	0	31(1)
O(12)	471(3)	−1841(2)	152(2)	37(1)
O(22)	1869(3)	28(2)	−1158(2)	40(1)
C(32)	2110(5)	1589(3)	1966(3)	36(1)
N(21)	2599(4)	−253(3)	−2846(2)	40(1)
C(12)	1816(5)	−2350(3)	281(3)	31(1)
C(22)	1759(5)	283(3)	−2062(3)	34(1)
C(23)	711(6)	1217(4)	−2446(3)	46(1)
C(24)	777(10)	952(8)	−3602(4)	109(3)
N(11)	1727(4)	−3551(3)	430(2)	36(1)
N(31)	3112(4)	1569(3)	2830(2)	42(1)
C(13)	3757(5)	−1772(4)	293(3)	43(1)
C(15)	3474(5)	−3928(4)	600(4)	49(1)
C(33)	1126(6)	2704(4)	2150(3)	49(1)
C(35)	2964(6)	2606(5)	3674(3)	58(1)
C(25)	2210(6)	173(5)	−3839(3)	55(1)
C(34)	1313(7)	3108(5)	3321(4)	67(1)
O(32)	2072(3)	795(2)	1161(2)	40(1)
C(26)	3776(5)	−1181(4)	−2767(3)	44(1)
C(36)	4307(5)	660(4)	2929(3)	45(1)
C(16)	72(5)	−4432(3)	442(3)	41(1)
C(14)	4769(6)	−2681(4)	712(5)	71(2)
C(60)	2271(10)	4709(7)	−3790(7)	113(2)
C(61)	2984(10)	5305(6)	−2767(6)	93(2)
N(62)	3550(14)	5821(8)	−1985(6)	158(3)
Cl(1)	2971(8)	7011(7)	3927(4)	61(1)
O(100)	4084(13)	6138(12)	4001(10)	161(5)
O(101)	1690(10)	6931(7)	4706(5)	120(2)
O(102)	1857(14)	6575(12)	3059(8)	149(4)
O(103)	3690(24)	8203(11)	4107(14)	234(8)
Cl(2)	3363(28)	7061(23)	3696(15)	99(7)
O(110)	2322(32)	7357(26)	2963(15)	124(12)
O(111)	3838(46)	8062(27)	4538(14)	147(13)
O(112)	5016(24)	7301(21)	3225(18)	139(9)
O(113)	3192(44)	6019(27)	4045(33)	213(17)

^{a} Equivalent isotropic *U* defined as one-third of the trace of the orthogonalized $\mathbf{U}_{ij}$ tensor.

Table 6. Atomic Coordinates ($\times 10^4$) and Equivalent Isotropic Displacement Coefficients (Å^2 $\times$ 10^3) for **5**

	x	*y*	*z*	*U*(eq)^a
Cd	5000	3104(1)	2500	45(1)
O(1)	6633(3)	3050(3)	3429(3)	57(2)
C(1)	7200(5)	3687(5)	3958(3)	42(3)
C(2)	6994(5)	4865(5)	4143(4)	60(3)
C(3)	7970(6)	5290(6)	4741(4)	81(4)
C(4)	8630(5)	4272(6)	5055(4)	62(3)
N(5)	8123(4)	3395(4)	4473(3)	43(2)
C(6)	8602(4)	2330(5)	4454(4)	49(3)
C(7)	9402(5)	2412(6)	4039(4)	53(3)
N(8)	8972(4)	2803(4)	3187(3)	48(2)
C(9)	8321(6)	2086(5)	2520(4)	64(3)
C(10)	8188(5)	2767(5)	1742(4)	62(3)
C(11)	8363(5)	3959(6)	2048(3)	63(3)
C(12)	8999(5)	3875(6)	2953(4)	50(3)
O(12)	9464(3)	4633(4)	3413(2)	65(2)
O(2)	5000	1236(5)	2500	56(3)
N(20)	4311(4)	3945(7)	3754(4)	73(3)
O(21)	4504(4)	4556(4)	3214(3)	81(2)
O(22)	4416(4)	2905(4)	3687(3)	71(2)
O(23)	4033(4)	4341(5)	4295(3)	108(3)

^{a} Equivalent isotropic *U* defined as one-third of the trace of the orthogonalized $\mathbf{U}_{ij}$ tensor.

influenced the ease with which these materials could be fully characterized.

Complexes of Mn−Zn: Halide Complexes. Complexes of stoichiometry MX_2(ebpyrr) were isolated with CoX_2 and ZnX_2 (X = Cl, Br, I). The deep blue cobalt complexes have solid state electronic spectra characteristic[10] of slightly distorted tetrahedral metal coordination, showing three strong, overlapping bands in the range 5000−8000 cm^{-1} [transitions to components of $^4T_1$(F)] and a strong multicomponent band centered on *ca.* 16 000 cm^{-1} [transitions to components of $^4T_1$(P)]. Additional evidence[11] for essentially tetrahedral MCl_2O_2 coordination in the compounds M(ebpyrr)Cl_2 (M = Co, Zn) comes from the ν_{asym}(M−X) and ν_{sym}(M−X) bands in their low-frequency IR spectra [343 and 304 cm^{-1} for M = Co; 338 and 302 cm^{-1} for M = Zn]. The low-frequency IR spectrum of the iron(III) chloride complex Fe(ebpyrr)Cl_3 has a very strong band at 379 cm^{-1} indicating[12] the presence of the $FeCl_4^-$ ion and the

---

(10) Goodgame, D. M. L.; Goodgame, M. *Inorg. Chem.* **1965**, *4*, 139.

(11) Nakamoto, K. *Infrared and Raman Spectra of Inorganic and Coordination Compounds*, 3rd ed.; Wiley: New York, 1977; Part III, pp 317−324 and references therein.

Table 7. Selected Bond Lengths (Å) and Angles (deg) for **1**

Co–Cl(1)	2.222(3)	Co–Cl(2)	2.224(3)
Co–O(1)	1.980(5)	Co–O(12)	1.984(5)
Cl(1)–Co–Cl(2)	119.1(1)	Cl(1)–Co–O(1)	103.9(2)
Cl(2)–Co–O(1)	114.2(2)	Cl(1)–Co–O(12)	109.6(2)
Cl(2)–Co–O(12)	105.5(2)	O(1)–Co–O(12)	103.6(2)
Co–O(1)–C(1)	133.0(5)	Co–O(12)–C(12)	126.8(5)

Table 8. Selected Bond Lengths (Å) and Angles (deg) for **2**

Zn–I(1)	2.553(1)	Zn–I(2)	2.570(1)
Zn–O(1)	2.000(4)	Zn–O(12)	1.975(5)
I(1)–Zn–I(2)	121.1(1)	I(1)–Zn–O(1)	105.8(1)
I(2)–Zn–O(1)	107.8(1)	I(1)–Zn–O(12)	114.6(1)
I(2)–Zn–O(12)	106.3(2)	O(1)–Zn–O(12)	98.8(2)
Zn–O(1)–C(1)	126.2(4)	Zn–O(12)–C(12)	137.4(5)

Table 9. Selected Bond Lengths (Å) and Angles (deg) for **3**

Co–O(12)	2.062(9)	Co–O(1)	2.063(11)
Co–O(31)	2.080(12)	Co–N(42)	2.11(3)
Co–O(22)	2.192(11)	Co–O(21)	2.203(14)
O(12)–Co–O(1)	92.3(4)	O(12)–Co–O(31)	170.8(7)
O(1)–Co–O(31)	83.6(5)	O(12)–Co–N(42)	89.3(5)
O(1)–Co–N(42)	100.9(6)	O(31)–Co–N(42)	99.6(6)
O(12)–Co–O(22)	81.6(4)	O(1)–Co–O(22)	152.7(7)
O(31)–Co–O(22)	98.3(4)	N(42)–Co–O(22)	105.5(7)
O(12)–Co–O(21)	85.3(4)	O(1)–Co–O(21)	94.3(5)
O(31)–Co–O(21)	86.8(5)	N(42)–Co–O(21)	164.0(5)
O(22)–Co–O(21)	58.8(6)	C(1)–O(1)–Co	128.3(13)
C(12)–O(12)–Co	140.6(8)	N(20)–O(22)–Co	92.8(12)
N(20)–O(21)–Co	91.2(14)	N(30)–O(31)–Co	120.5(14)
C(41)–N(42)–Co	172(2)		

Table 10. Selected Bond Lengths (Å) and Angles (deg) for **4**

Zn–O(12)	2.107(2)	Zn–O(22)	2.104(2)
Zn–O(32)	2.112(2)		
O(12)–Zn–O(22)	88.46(9)	O(12)–Zn–O(22a)	91.54(9)
O(12)–Zn–O(32)	90.34(10)	O(12)–Zn–O(32a)	89.66(10)
O(22)–Zn–O(32)	90.58(10)	O(22)–Zn–O(32a)	89.42(10)
O(12)–Zn–O(12a)	180.0	O(22)–Zn–O(22a)	180.0
O(32)–Zn–O(32a)	180.0	C(12)–O(12)–Zn	135.9(2)
C(22)–O(22)–Zn	131.3(2)	C(32)–O(32)–Zn	131.8(2)

Table 11. Selected Bond Lengths (Å) and Angles (deg) for **5**

Cd–O(1)	2.290(4)	Cd–O(2)	2.228(6)
Cd–O(21)	2.351(6)	Cd–O(22)	2.437(6)
Cd–O(1a)	2.290(4)	Cd–O(21a)	2.351(6)
Cd–O(22a)	2.437(6)		
O(1)–Cd–O(2)	88.4(1)	O(1)–Cd–O(21)	93.3(2)
O(2)–Cd–O(21)	137.4(1)	O(1)–Cd–O(22)	87.2(2)
O(2)–Cd–O(22)	84.4(1)	O(21)–Cd–O(22)	53.3(2)
O(1)–Cd–O(1a)	176.8(2)	O(2)–Cd–O(1a)	88.4(1)
O(21)–Cd–O(1a)	89.1(2)	O(22)–Cd–O(1a)	92.5(2)
O(1)–Cd–O(21a)	89.1(2)	O(2)–Cd–O(21a)	137.4(1)
O(21)–Cd–O(21a)	85.1(3)	O(22)–Cd–O(21a)	137.9(2)
O(1a)–Cd–O(21a)	93.3(2)	O(1)–Cd–O(22a)	92.5(2)
O(2)–Cd–O(22a)	84.4(1)	O(21)–Cd–O(22a)	137.9(2)
O(22)–Cd–O(22a)	168.8(2)	O(1a)–Cd–O(22a)	87.2(2)
O(21a)–Cd–O(22a)	53.3(2)	Cd–O(1)–C(1)	136.6(4)
Cd–O(21)–N(20)	97.1(5)	Cd–O(22)–N(20)	93.4(5)

formulation of the complex as [Fe(ebpyrr)$_2$Cl$_2$][FeCl$_4$], as found for the iron(III) chloride complexes with some other O-donor ligands.[5,13]

The longer range geometries present in two members of this group of compounds, Co(ebpyrr)Cl$_2$ (**1**) and Zn(ebpyrr)I$_2$ (**2**), were determined by X-ray diffraction studies.

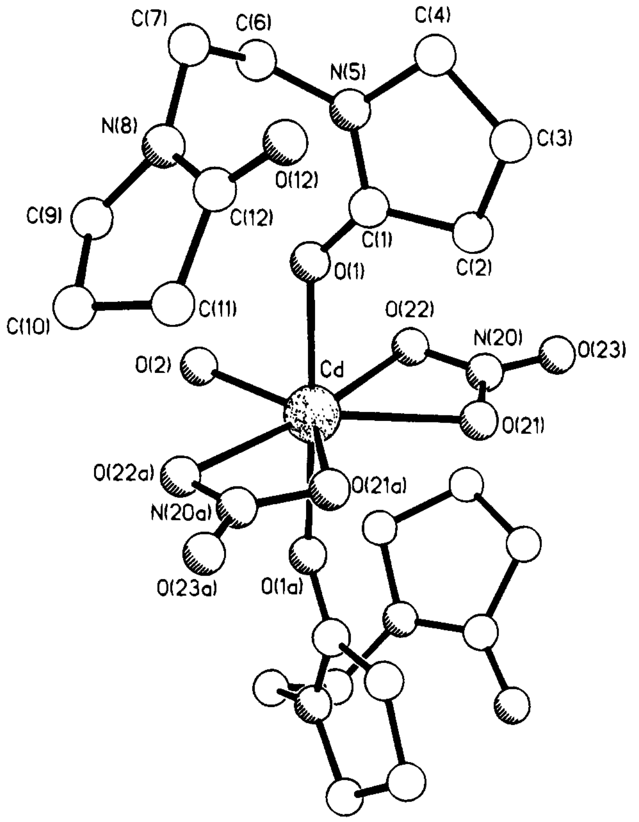

Figure 6. Molecular structure in the crystals of compound **5**, showing the crystallographic numbering scheme.

Structure of Co(ebpyrr)Cl$_2$ (1). The X-ray study of **1** shows that each cobalt ion is tetrahedrally coordinated to two chlorides and two oxygen atoms, one from each of two ebpyrr ligands (Figure 1). The Co–Cl bonds [2.222(3) and 2.224(3) Å] are essentially equivalent, as are the Co–O bonds [1.980(5) and 1.984(5) Å]. The distortion of the tetrahedron, indicated by the electronic spectrum, is also reflected in both the bond angles (the Cl–Co–Cl angle is expanded to 119.1°, and the O–Co–O angle is somewhat contracted to 103.6°) and in a 4° twist about the C_2 axis that bisects the Cl(1)–Co–Cl(2) angle.

The ebpyrr ligands serve to bridge cobalt ions to form helical chains (Figure 2) with the chain being propagated by the 2_1 screw axis along the crystallographic *b* direction; there is a separation of 6.1 Å between adjacent cobalt centers. The –NCH$_2$CH$_2$N– bridge unit has *gauche* geometry (67° N–CH$_2$–CH$_2$–N torsion angle). The torsional twists about the N(5)–C(6) and C(7)–N(8a) bonds are *ca.* 80 and 84°, respectively. This arrangement is essentially the same as that found for the complex [UO$_2$(ebpyrr)(NO$_3$)$_2$]$_n$.[3] The helical chains are essentially hexagonally close-packed (Figure 3); there are no significant interhelix interactions.

Structure of Zn(ebpyrr)I$_2$ (2). The X-ray study of **2** reveals that it also forms a chain-polymer structure in which the ebpyrr ligands bridge tetrahedrally coordinated zinc atoms (Figure 3), with a Zn–Zn separation of 6.6 Å within the chain. The tetrahedral geometry in **2** is more distorted than that in **1**; the I–Zn–I angle is 121.1(1)° and the O–Zn–O angle [98.8(2)°] is significantly compressed. There is again a C_2 twist distortion of *ca.* 4°.

The direction of the chain propagation is along the crystallographic 101 direction. In contrast to **1**, the chains in **2** are not helical; the iodide ions all lie on one side of the chain (the structure being polar). The ebpyrr ligand geometry, however, does not differ markedly from that observed in **1**. There is a *ca.* 69° torsion twist about the C(6)–C(7) ethylene bond and

---

[12] Avery, J. S.; Burbridge, C. D.; Goodgame, D. M. L. *Spectrochim. Acta, Part A* **1968**, *24*, 1721.

[13] See, for example: Durcanská, E.; Glowiak, T. *Acta Crystallogr., Sect. C* **1989**, *45*, 410. Povey, D. C.; Lobana, T. S.; Bhatia, P. K. *J. Crystallogr. Spectrosc. Res.* **1991**, *21*, 13.

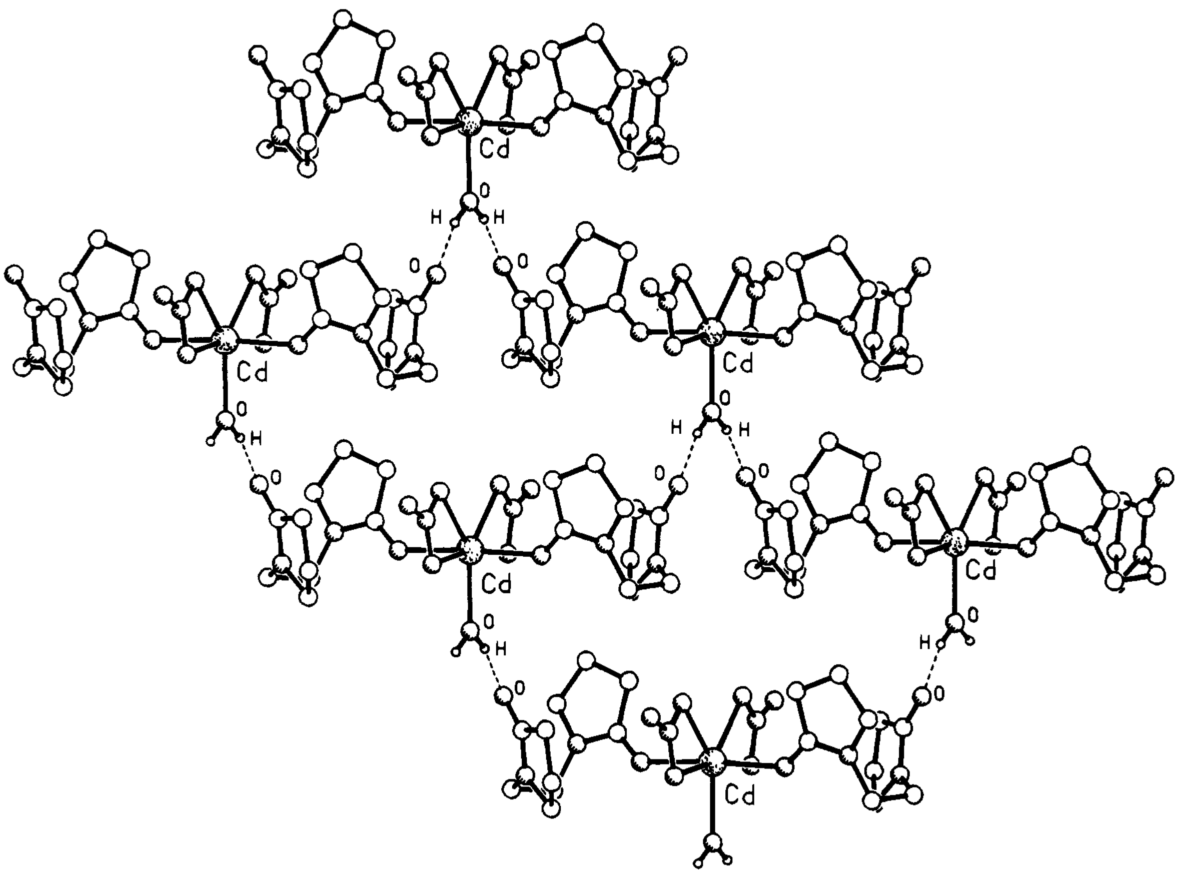

Figure 7. Linking of the [Cd(NO$_3$)$_2$(ebpyrr)$_2$(H$_2$O)] molecules into sheets via hydrogen bonding in the crystals of **5**.

Scheme 1

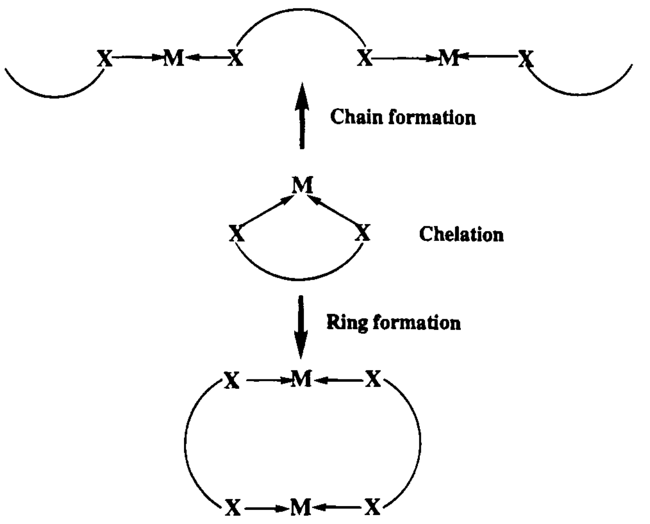

twists of 66 and 85° about C(7)−N(8a) and C(6)−N(5), respectively, producing a transoid relationship of the two ligand carbonyl groups. It is this ligand geometry in both **1** and **2** that favors the chain formation. The chains in **2** are also in a hexagonally close packed arrangement within the crystal, as shown in Figure 4, which also highlights the polar nature of the structure. The chains are relatively loosely packed; the closest interchain contact (3.17 Å) is between I(1) and a hydrogen atom, H(7), in an ethylene bridge.

The change from a helical-chain structure in **1** to the nonhelical, polar chain in **2** merits comment. Clearly, the difference is not a consequence of the organic ligand conformation which exhibits only minor differences between the two structures. An analysis of the terminal angles about the metal−oxygen and carbonyl bonds reveals that those about the latter are essentially unchanged on going from **1** to **2**, the metal in each case lying close to the pyrrolidone ring plane. The rotation about one of the metal−oxygen bonds is also the same in both structures [O(12)CoO(1)C(1) = −115°, and O(1)ZnO(12)C(12) = −113°]. However, the rotation about the other metal−oxygen bond is distinctly different, with a rotation of 47° in the cobalt structure but one of −174° in the zinc complex.

The X-ray powder pattern of [Co(ebpyrr)I$_2$] shows that it is isomorphous with **2**, but that of [Zn(ebpyrr)Cl$_2$] differs from that of its cobalt analogue, **1**.

The formation of chain structures by these compounds differs from the discrete dinuclear metallocycles formed by the cobalt bromide complex with the thio analogue of ebpyrr (**IV**),[14] by [Co(EBP)Cl$_2$]$_2$ [where EBP = *N,N'*-ethylenebis(pyridine-2-one)],[15] and by [Zn(*o*-XBP)Cl$_2$]$_2$ [where *o*-XBP = *N,N'*-*o*-phenylenedimethylenebis(pyridin-2-one)].[5] As indicated schematically in Scheme 1, either of these structural types would be expected as a possible product when the chelation of the "extended reach" ligand becomes disfavored. The choice between chain or individual ring is likely to involve a number of factors, e.g. the nature of the ring donor units and their respective orientations (e.g. cisoid or transoid), the bridge between them, the metal ion, counteranions, and the solvent employed. Indeed, it is likely that structural isomers (chains or rings) may be obtained by appropriate choice of experimental conditions, but confirmation of this depends critically on the formation of crystalline samples for X-ray characterization.

The dominant metal-containing species in the FAB mass spectra of **1** and **2** were, in each case, the ions [MX(ebpyrr)]$^+$

---

(14) Atherton, Z.; Goodgame, D. M. L.; Katahira, D. A.; Menzer, S.; Williams, D. J. *J. Chem. Soc., Chem. Commun.* **1994**, 1423.

(15) Hill, S. P. W. Ph.D. Thesis, London University, 1993.

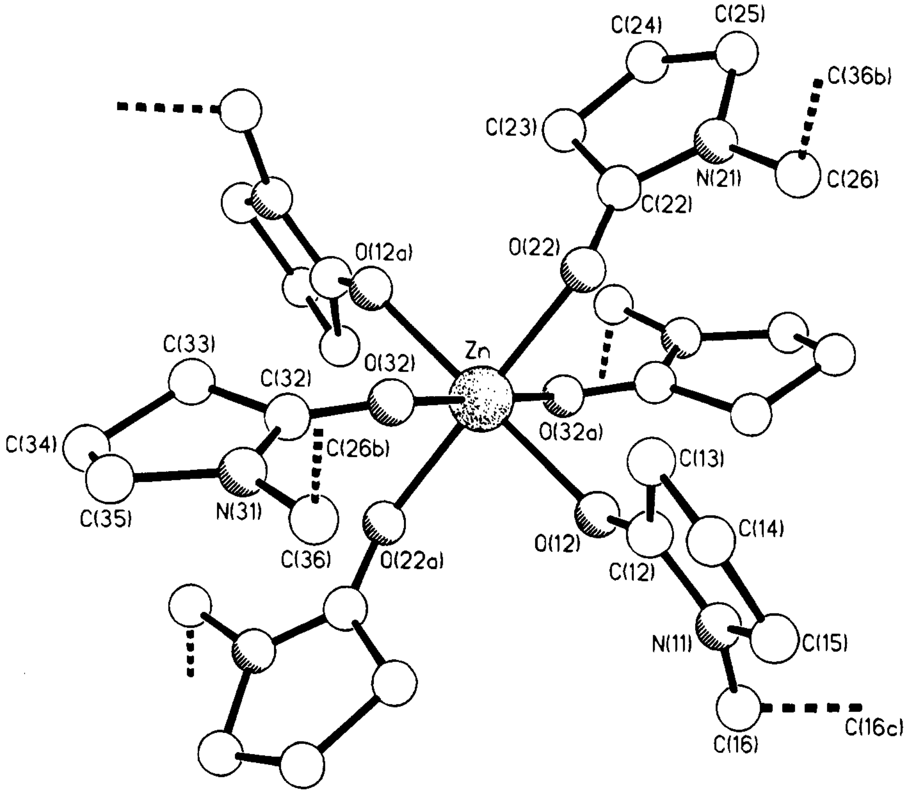

Figure 8. Zinc coordination environment in compound **4**, showing the crystallographic numbering scheme.

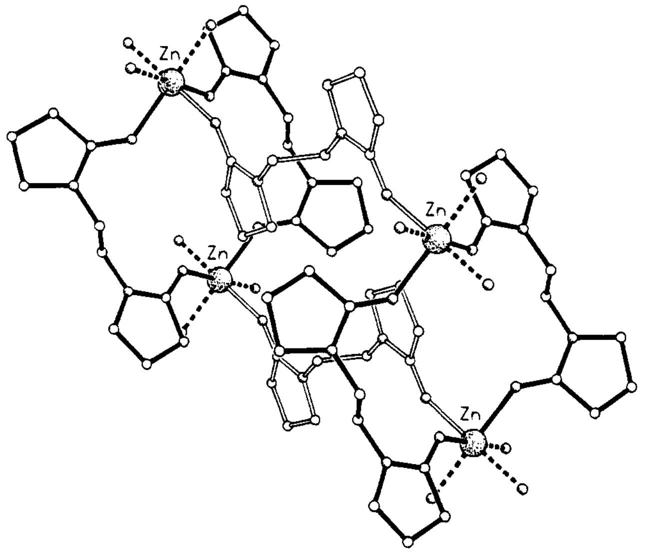

Figure 9. Linking of 16-membered rings (shown with filled bonds) by pairs of type B ebpyrr bridges (shown with unshaded bonds), and the consequent formation of 36-membered rings, in the structure of **4**.

and $[MX(ebpyrr)_2]^+$, and only in the case of **1** were fragments of higher nuclearity, $[Co_2Cl_3(ebpyrr)_2]^+$ and $[Co_3Cl_5(ebpyrr)_2]^+$, observed and then in minor abundance.

Transition Metal Nitrate Complexes. Using acetonitrile as solvent, hydrated manganese(II) nitrate readily gave a complex of stoichiometry $Mn(NO_3)_2(ebpyrr)_2\cdot H_2O$, but the complexes $M(NO_3)_2(ebpyrr)$ (M = Co–Zn) were found to be very hygroscopic, and they could only be satisfactorily isolated by using 2,2-dimethoxypropane or mixed 2,2-dimethoxypropane/acetonitrile solvent systems. The Co and Ni compounds had electronic spectra indicative of essentially octahedral coordination. Full characterization of this group of compounds was hampered by difficulties in obtaining good crystals. Some small crystals of $Co(NO_3)_2(ebpyrr)\cdot CH_3CN$ (**3**) were obtained, and these were characterized by X-ray diffraction methods.

Structure of $Co(NO_3)_2(ebpyrr)\cdot CH_3CN$, 3. The crystals of **3** proved to be very unstable, desolvating instantly on removal from solution. After several attempts, a partial crystallographic data set was obtained for a crystal coated with epoxy resin; the crystal had decomposed by *ca.* 50% after only one-third of a total data set had been collected. Despite these limitations, a definitive structure solution was achieved, though its limited accuracy precludes full discussion.

Each cobalt atom in **3** is octahedrally coordinated, with the metal being bonded to one monodentate nitrate, one bidentate nitrate, an acetonitrile molecule, and an oxygen atom from each of two ebpyrr ligands (Figure 5). The ebpyrr ligands bridge adjacent cobalt centers, forming a chain extending in the crystallographic *c* direction (Co··Co 7.9 Å). The conformation of the ebpyrr bridge is very similar to that in **1** and **2**, with a *gauche* geometry about the C(6)–C(7) linkage and a retention of approximate coplanarity of the metal atom with respect to its adjacent pyrrolidone ring plane. The chain in **3** is nonhelical; the acetonitriles and the monodentate nitrates all lie on one side of the chain.

The chains pack with their longitudinal axes parallel, so as to form sheets extending in the crystallographic *b* and *c* directions, with the acetonitrile ligands and the monodentate nitrates forming one "face" of each sheet. Adjacent sheets stack so that these surfaces are in a face-to-face arrangement.

The coordinated acetonitrile molecules are lost extremely readily, and exposure to atmospheric water results in rapid loss of crystallinity and the formation of a pink complex analyzing[16] as $Co(ebpyrr)(NO_3)_2(H_2O)$. It seems likely that during this process the water molecule coordinates in place of the acetonitrile, but the loss of crystallinity precludes X-ray confirmation.

Structure of $Cd(NO_3)_2(ebpyrr)_2\cdot H_2O$, 5. Reaction of ebpyrr

---

[16] Anal. Calc for $Co(ebpyrr)(NO_3)_2(H_2O)$: C, 30.2; H, 4.6; N, 14.1. Found: C, 30.0; H, 4.5; N, 13.9.

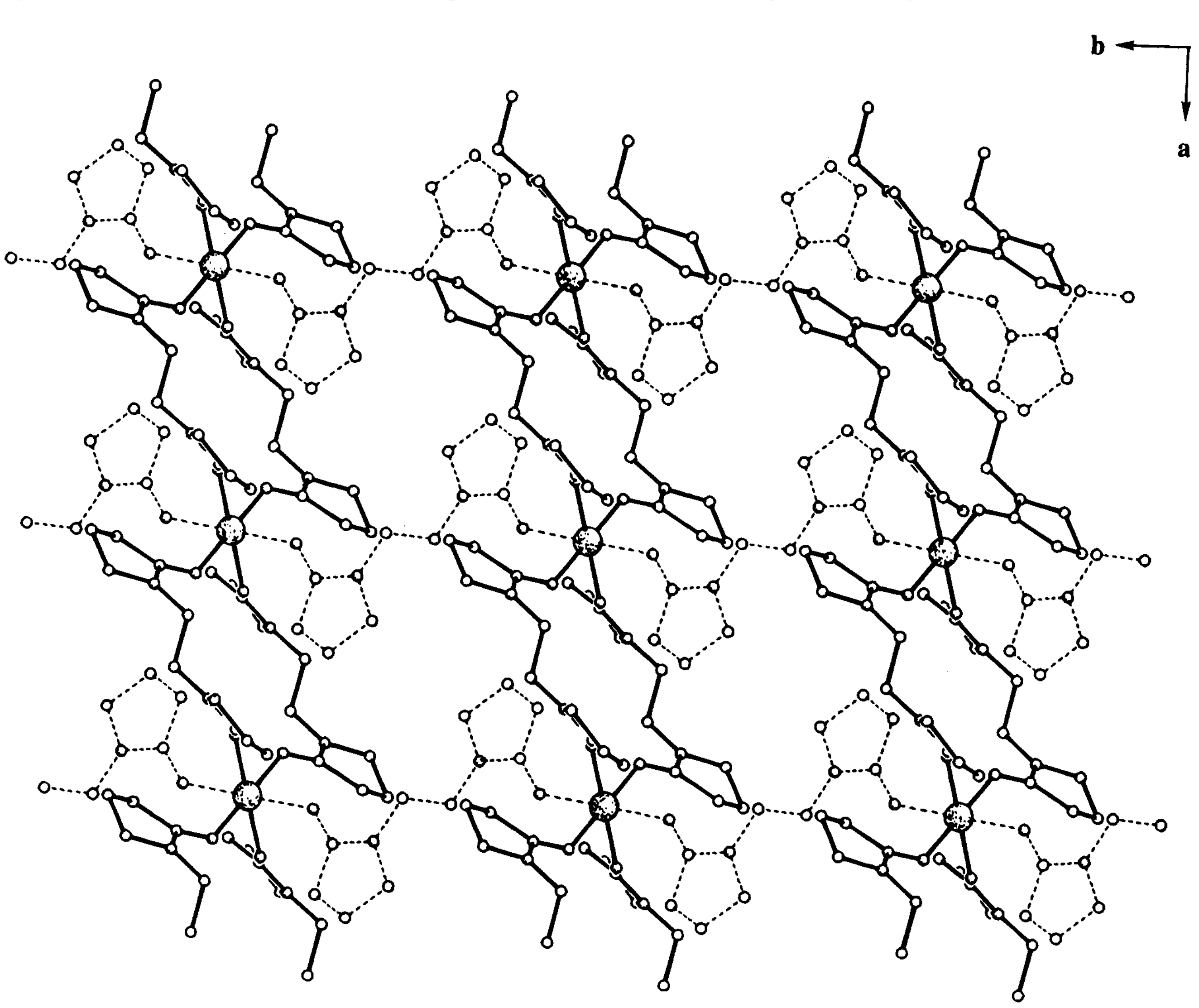

Figure 10. View normal to the *ab* plane in the crystal structure of **4** showing how the chains of 16-membered rings (shaded bonds) are connected by sets of type B ebpyrr bridges (dotted bonds) so as to form sheets extending in the *ab* plane.

with cadmium nitrate in 2:1 mole ratio in 2,2-dimethoxypropane afforded the compound $Cd_2(NO_3)_4(ebpyrr)_3$ as very small white needles. Attempts to obtain X-ray quality crystals by varying the solvent (see Experimental Section) eventually resulted in the formation of colorless cubes, **5**. However, the X-ray diffraction study of **5** showed that these crystals were of a compound of stoichiometry $Cd(NO_3)_2(ebpyrr)_2{\cdot}H_2O$.

The complex is mononuclear (Figure 6). Each cadmium atom is bonded to seven oxygen atoms, one from each of two ebpyrr molecules, the oxygen atom of the aqua ligand, and four oxygens from two chelating nitrate groups (the Cd–O bond lengths to each nitrate group are 2.351(7) and 2.429(8) Å, respectively). The coordination geometry about the Cd atom is essentially pentagonal bipyramidal with the oxygen atoms from the ebpyrr ligands occupying the axial positions [O(1)–Cd–O(1a) 176.8(2) Å] and the nitrate groups and the aqua ligand forming the equatorial plane. The molecule has crystallographic C_2 symmetry about the Cd–O(2) axis. The maximum deviation from planarity of the atoms within the equatorial plane is 0.03 Å. The angles within the equatorial CdO_5 unit range from 53 to 85°, the departure from the idealized pentagonal bipyramidal angle reflecting the constraints of the "bite" of the chelating nitrate groups. One could alternatively regard the coordination geometry as based on a trigonal bipyramid with each nitrate group occupying one equatorial coordination position and the aqua ligand the third; the O(2)–Cd–N(nitrate) angles are 111°, and the N(nitrate)–Cd–N(nitrate) angle is 138°.

The Cd coordination geometry in **5** is very similar to that recently reported[17] for $\{[Cd_2(\mu\text{-bpe})_3](NO_3)_4\}_n$ [bpe = 1,2-bis(4-pyridyl)ethane], which has two bidentate nitrates and a pyridyl nitrogen in the equatorial positions and two pyridyl groups in the axial positions. That compound, however, forms a chain of $[Cd_2(\mu\text{-bpe})_2]$ rings connected by bpe bridges, analogous to the structure previously reported for the compound $[Hg_3Tb_2L_6(NO_3)_6]_n$ (L = the anion[18] of 2-pyrrolidone).

The ebpyrr ligand geometry in **5** differs little from that observed in **1**, with a *gauche* geometry about the C(6)–C(7) bond (60°) and mean torsion angles about the N(5)–C(6) and C(7)-N(8) bonds of 77 and 78°, and a *transoid* relationship of the terminal carbonyl bonds.

In contrast to the chain structures observed for **1**, **2**, and **3**, in **5** adjacent $[Cd(NO_3)_2(ebpyrr)_2(H_2O)]$ molecules are connected via hydrogen bonds between the aqua ligand and the noncoordinated oxygen atoms, O(12) and O(12a), respectively, of the ebpyrr ligands [O(2)–H···O(12) = 2.73 Å, H···O(12) = 1.77 Å, O–H···O angle = 162°] to form extended sheets (Figure

---

(17) Fujita, M.; Kwon, Y. J.; Miyazawa, M.; Ogura, K. *J. Chem. Soc., Chem. Commun.* **1994**, 1977.

(18) Goodgame, D. M. L.; Williams, D. J.; Winpenny, R. E. P. *J. Chem. Soc., Dalton Trans.* **1989**, 1439.

7). It is probably the coordination of this water molecule, under the solvent conditions required for the crystal formation, which appears to frustrate the formation of directly linked chains or more extended sheets, though, from the stoichiometry, these may well be present in the compound $Cd_2(NO_3)_4(ebpyrr)_3$.

Structure of $[Zn(ebpyrr)_3](ClO_4)_2{\cdot}2MeCN$ (4). The hydrated perchlorates of Mn(II), Co(II), and Zn(II) gave complexes of the type $[M(ebpyrr)_3](ClO_4)_2$, and zinc tetrafluoroborate formed the compound $[Zn(ebpyrr)_3](BF_4)_2.MeCN$. Crystals of X-ray quality were obtained from acetonitrile solution for the zinc perchlorate complex, **4**, and this member of the series was fully characterized by X-ray diffraction methods.

The X-ray study showed that the crystalline sample of **4** had the stoichiometry $[Zn(ebpyrr)_3](ClO_4)_2{\cdot}2MeCN$. Each zinc atom lies on a crystallographic center of symmetry and is octahedrally coordinated by six oxygen atoms, one from each of six different ebpyrr ligands (Figure 8). The Zn−O bond lengths are in the range 2.104(2)−2.112(2) Å, and the O−Zn−O bond angles are in the range 88.45(9)−91.55(9)°. The ebpyrr ligands bridge adjacent zinc centers and adopt two different conformations. In both, the ethylene bridge adopts an *anti*-geometry, but in one (type A) the carbonyl groups are oriented in an approximately *gauche*-geometry (O=C··C=O torsion angle = 48°), while in the other (type B) these groups are *anti* with respect to each other (there is a center of symmetry at the center of the ethylene bridge). In both A and B bridges, the CH_2-CH_2 bond is strongly inclined to the pyrrolidone ring plane (68 and 82° in type A and 63° in type B).

Pairs of type A bridges serve to link adjacent zinc atoms, forming 18-membered rings. These, in turn, are linked by type B bridges, forming an additional set of 36-membered rings, as shown in Figure 9. The 18-membered rings propagate to form chains that extend in the crystallographic *a* direction. The cross-linking by type B bridges generates sheets extending in the crystallographic *ab* plane (Figure 10). Within the 18-membered rings the transannular Zn−Zn distance is 7.53 Å, and in the 36-membered ring the shorter transannular Zn−Zn distance is 12.18 Å.

The crystallographic study also revealed that the perchlorate ions and the two molecules of acetonitrile of solvation per zinc center in the crystals of **4** are located between the $[Zn(ebpyrr)_3]_n$ layers.

Table 12. Phosphorescence Emission Data for Solid Samples of $[M_2(ebpyrr)_3(NO_3)_6]_n$ (M = Sm, Eu, Tb, or Dy)

M	excitation, nm	phosphorescent emission, nm	lifetime, μs^a
Sm	405	563 ($^4G_{5/2} \rightarrow {}^6H_{5/2}$), 599 ($^6H_{7/2}$), 643 ($^6H_{9/2}$)	35
Eu	398	594 ($^5D_0 \rightarrow {}^7F_1$), 618 ($^7F_2$)	1400
Tb	320	491 ($^5D_4 \rightarrow {}^7F_6$), 545 ($^7F_5$), 585 ($^7F_4$), 622 ($^7F_3$)	1450
Dy	366	482 ($^4F_{9/2} \rightarrow {}^6H_{15/2}$), 574 ($^6H_{13/2}$)	40

[a] Measured for the 599 nm band (Sm), 618 nm band (Eu), 545 nm band (Tb), and 574 nm band (Dy).

Lanthanide Complexes. In a preliminary communication[1] we described the structure of the acetonitrile solvate of the compound $[Er_2(ebpyrr)_3(NO_3)_6]_n$, **6**. The rest of the lanthanide(III) nitrates from Pr to Yb (promethium and lutetium not studied) and yttrium(III) nitrate form analogous complexes. The formation of the same stoichiometry does not, of course, necessarily imply retention of the same structure across the lanthanide series, so X-ray powder diffraction studies were carried out on two further, representative members (the Nd and Dy compounds) for comparison with that of **6**. These showed that the Nd and Dy complexes have basically the same structure as that of the Er compound, though there was evidence of a varying degree of solvent inclusion. (As stated previously, all members of this set of compounds rapidly lose their acetonitrile molecules of solvation once the crystals are removed from solution.)

Four of the solid lanthanide nitrate complexes $[Ln_2(ebpyrr)_3(NO_3)_6]_n$ (Ln = Sm, Eu, Tb, Dy) luminesce under near-UV excitation, and their phosphorescent emission properties are summarized in Table 12.

The stoichiometry of the thorium(IV) nitrate complex $Th_2(NO_3)_8(ebpyrr)_3$ suggests that it may also be polymeric, but crystals of X-ray quality could not be obtained.

Acknowledgment. We thank the SERC for a Research Studentship (to S.P.W.H.) and for the diffractometer and the CEC for a Visiting Fellowship (to S.M.).

Supplementary Material Available: Tables giving details of the crystallographic data collection, a full set of bond lengths and angles, anisotropic displacement coefficients, and H atom coordinates and displacement coefficients (31 pages). Ordering information is given on any current masthead page.

IC9413878